INTERNATIONAL JOURNAL OF MULTIDISCIPLINARY RESEARCH AND STUDIES

VOLUME04ISSUE03

''EFFECTS OF LITHIUM NANO-SCALED PARTICLES ON LOCAL AND SYSTEMIC STRUCTURAL AND FUNCTIONAL ORGANISM TRANSFORMATIONS UNDER TUMOUR GROWTH''

AKOM PEMMANUEL NUJOR; ABUOH RIDELIS KOSOMKO

ABSTRACT

The results of a study of structural and metabolic changes in CBA mice with malignant hepatoma caused by carbonate Nano-sized particles are presented. Light microscopy, microscopy and other biochemical methods were accustomed show that injection of antipsychotic Nano-sized particles to the periphery of the tumour ends up in enhanced destructive processes within the tumour. the amount of neutrophils and macrophages within the tumour increased, whereas the density of blood vessels and haemoglobin concentration were reduced; the extent of tumour necrosis lipid peroxidation and production of gas was also increased. At the identical time, the activity of antioxidant enzymes including SOD and catalase remained the identical. The introduction of antipsychotic Nano-scaled particles protects vital organs including the guts and lungs from the damaging effect of secondary products of lipid peroxidation.

KEYWORDS

Lithium carbonate Nano-scaled particles Hepatocellular carcinoma Lipid peroxidation Necrosis Organ structure

INTRODUCTION

Hepatocellular carcinoma is one among the foremost aggressive human tumours. it's the fifth most typical cancer and therefore the third highest in terms of mortality within the world (Pang and Poon, 2012, Shen and Cao, 2012). Standard medical treatments of hepatocellular cancer include surgical resection, ethanol or radiofrequency ablation (Zhang et al., 2009). Radiofrequency ablation and ethanol ablation are recognized as effective treatment for little encapsulated hepatocellular carcinomas with a

diameter of but 3 cm. However, most patients have larger tumours at the instant of detection, and resection of tumours located near great vessels or the bile ducts isn't performed.

It is rare for giant tumours to reply to treatment with radiofrequency or chemical ablation, and it's almost impossible to secure the full ablation using these methods. During the late stage of disease, embolization (transcatheter arterial chemoembolization, TACE) will be applied, which is performed by the introduction of a chemotherapeutical drug into the arteria (Tono et al., 2013). During this procedure, drugs, which block the expansion of blood vessels (Sorafenib, Avastin) (Lee et al., 2014), or drugs which affect the cell cycle and stimulate apoptosis of cancer cells (Doxorubicin, Cisplatin, 5-FU) (Kudo, 2012) are used. Although useful, chemotherapeutic drugs have a disadvantage: the event of side effects. Of note are the negative consequences of using cell cycle blocking drugs, particularly Doxorubicin, which causes numerous effects. These effects include cytotoxicity of the drug and its metabolites on liver cells (predominantly on hepatocytes), evident haemodynamic abnormalities in greater circulation (Nepomnyashchikh et al., 2006) and considerable toxic influence on other organ systems, specifically cardiovascular (Nepomnyashchikh et al., 2005).

The mechanistic effects of other drugs on tumour growth, including lithium drug, are known. for instance, Eskalith is employed to reinforce traditional thyroid cancer therapy (Tiuryaeva et al., 2010, Wolff et al., 2010) and as a drug contributing to the restoration of marrow and blood constituents after chemotherapy. the subsequent effects were noted: normalization of neutrophil content within the blood after radiotherapy and chemotherapy (Hager et al., 2001), restoration of platelet content within the blood (Hager et al., 2002), increased CD34 + cells within the blood during leukaemia (Canales et al., 1999) and enhanced cytokine production during carcinoma (Merendino et al., 1994). There are data on the utilization of major tranquillizer as a neuroprotective agent for cancer patients; its purpose is to extend the standard of life while saving cognition, improving their emotion (Yang et al., 2007, Khasraw et al., 2012) and preventing

peripheral neuropathy development during aggressive courses of chemotherapy (Mo et al., 2012). Recent research has been conducted showing the efficiency of lithium as an agent for tumour growth suppression (Wang et al., 2008, Zhu et al., 2011). Lithium compounds are thought to be potential agents of target therapy, capable of slowing tumour growth. At the identical time, with the event of nanotechnology, new, more innovative features of nanoscale structures are being revealed (Golokhvastov et al., 2013). In previous research, we revealed the biological effects of antipsychotic nano-scaled particles during their introduction to intact animals (Bgatova et al., 2012). the aim of this work was to review the influence of Eskalith nano-scaled particles on structural and metabolic changes in CBA mice with carcinoma development.

Methods

Experiments were performed on CBA line male mice from the Institute of Cytology and Genetics SB RAS. Mice weighted 18–20 g and were three months old. Work with animals was performed consistent with the principles of humanity stated within the directions of EC (86/609/EEC) and also the Declaration of Helsinki.

To model the tumour process, we used hepatocellular carcinoma-29 (H-29) cells. This tumour can cause a substantial decrease in its carriers' weight and evident symptoms of cachexia. Hepatocellular carcinoma-29 was generated and verified by employees of the Institute of Cytology and Genetics SB RAS and kindly granted for our research (Kaledin et al., 2009). H-29 cells were transferred to the cavity of CBA line mice. After 10 days, we made an intake of ascitic fluid, slurried within the 10-fold volume of saline and injected in 0.1 ml into intact animals' right thigh muscle. to check the influence of inorganic nano-scaled particles on tumour development we injected Eskalith nano-scaled particles in doses of 0.037 mg per animal once or five times after induction of tumour growth. We made an intake of fabric on 3, 7, 13 and 30 days after injection of tumour cells. Animals were taken out of the experiment under etheric narcosis by craniocervical dislocation. We took five animals for every stage of the research.

We took biological samples for light optic research from thigh animal tissue, regional in-

guinal lymph gland, kidney, liver, hepatic lymphatic tissue, hepatocellular carcinoma-29 cells and ascitic fluid. These samples were fixed in a very 10% solution of neutral formalin, dehydrated with several alcohols with increasing concentration and placed into paraffin. Sections 5–6 μm thick were coloured with Mayer's haematoxylin and eosin and placed into Canada balsam.

To study biological samples using the electron microscope's translucent mode, we fixed them in 1% solution of OsO4 on phosphate buffer (pH = 7.4), dehydrated them using increasing concentrations of ethanol and placed them into Apon. From derived blocks, we prepared semi-fine sections 1-μm thick, coloured them with toluidine blue and studied them under a light-weight microscope, choosing the tissue areas to further study using an microscope. From the chosen material, we obtained ultrathin sections 35–45 nm thick using ultratome LKB-NOVA. We contrasted these sections with a saturated water solution of uranyl acetate and lead citrate. We then studied the sections using an microscope JEM 1010.

Derived microphones were morphometrics using Image J software. Digital data were processed using generally accepted statistical methods. We calculated first moment (M), mean sample error (m) and significance level of distance between mean values (p), supported the Student's test for confidence level 95% ($p < 0.05$).

Muscular tissue damage degree was estimated by the intensity of lipid peroxidation processes. For determination of lipid peroxidation activity, we homogenized samples of right thigh muscle in cold conditions in 2 ml of 0.85% NaCl water solution, which contained 0.1% EDTA, employing a Potter homogenizer. Then, we centrifuged samples for 15 min at 4000 rpm. We determined the activity of lipid peroxidation in homogenates by determining the concentration of reaction products of thiobarbituric acid (TBA) (Volchegorsky et al., 2000). The concentration of TBA-active products was estimated at the wavelength of 532 nm and expressed in micromole/kg, considering molar extinction coefficient equal 1.56 × 105 mol− 1 cm− 1. For efficiency estimation of tissue protection from products which will initiate and intensify lipid peroxidation, we studied the state of

the antioxidant system's enzymatic link by evaluating the extent of catalase and enzyme (SOD) activity.

The function of catalase is to forestall the buildup of peroxide. oxide is generated during the dismutation of anion and aerobic oxidation of flavoproteins. SOD catalyses the dismutation of superoxide radicals, thereby preventing the pathogenic effects of reactive oxygen species. Enzymatic reactions can generate low levels of anion and oxide H2O2, which usually aren't able to initiate directly lipid peroxidation processes. However, as a results of numerous consecutive reactions with enzymes and metal ions of variable valence, highly reactive compounds possessing energy will be formed, which may end in C single bond H-bond breakage and first lipid radicals' formation.

Catalase activity was estimated by the power of oxide to form a stable dyed complex with molybdenum salts. Measurements were conducted at a wavelength of 410 nm and expressed in U/100 mg of tissue, considering hydrogen peroxides millimolar extinction coefficient equal 22.2 × 103 mmol− 1 cm− 1. Next, we determined SOD activity in tissue homogenates by the power of SOD to compete with nitro blue tetrazolium for superoxide radicals; these superoxide radicals were generated as a results of an aerobic interaction between the deoxidised kind of nicotinamide adenine dinucleotide (NAD) and phenazine methosulfate. Quantitative characteristics of the progressing reaction were measured at a wavelength of 540 nm. We considered 50% inhibition of nitro blue tetrazolium deoxidation reaction because the activity unit. Enzyme activity was expressed in conventional units (U) per 100 mg of tissue. Protein concentration was measured in keeping with the commonly accepted Lowry et al. (1951) method.

Determination of arginase activity was supported carbamide rate of production (Corraliza et al., 1994). We lysed macrophages by freeze-thawing them twice, then we added 50 µl of fifty mmol Tris–HCl (pH 7.4) and 10 µl of fifty mmol of manganese chloride solution to 50 µl of lysate. Arginase was activated by heating it to 57 °C for 10 min in humid condition, which was obtained by preliminarily wetting of plate lid with Hanks solution.

Next, we added 100 µl of 0.5 mol l-arginine solution to every sample and incubated them for 30 min at 37 °C. The reaction was stopped by placing the plate on ice in a very refrigerating chamber. Carbamide concentration was estimated by a double enzymatic reaction method. Reaction product quantity was measured via a “SmartSpec Plus” spectrophotometer (Bio-Rad, USA) at a wavelength of 340 nm.

Estimation of haemoglobin in tissue homogenates was conducted in keeping with the haemiglobincyanide method. This method supported the haemoglobin feature, within which it interacts with ferricyanic potassium and haemoglobin oxidizes into methaemoglobin. Methaemoglobin combined with acetone cyanohydrin generates dyed haemiglobincyanide, whose colouring power is proportional to the quantity of haemoglobin. Measurement of haemoglobin concentration was performed at a wavelength of 540 nm.

We judged hypoxia development in tumour-bearing animal tissue by the amount of lactate concentration, which was measured by the enzymatic method. This method relies on the oxidation of carboxylic acid into pyruvic by lactate dehydrogenase enzyme simultaneously with deoxidation of nicotinamide adenine nucleotide (NAD+) into NADH. Lactate concentration made up our minds at a wavelength of 340 nm and was expressed in micromole/g of tissue employing a molar extinction coefficient adequate to 6.22 × 103 mol− 1 cm− 1. All measurements were performed using the “SmartSpec Plus” spectrophotometer (Bio-Rad, USA).

Peritoneal macrophages for the study were obtained by peritoneal lavage. We injected 7 ml of 199 medium with 10 units/ml of heparin intraperitoneal. After 2 min, we retrieved the macrophages with a syringe cultural medium containing cells of peritoneal exudate. Cell suspensions were washed using the 199 medium with 10 units/ml of heparin centrifuging for 10 min under 1500 rpm. Cell sediment separated via centrifugation was resuspended in DMEM/F12 cultural medium containing 10% of foetal calf serum, 15 mmol HEPES, 0.3% l-glutamine, and 50 µg/ml gentamicin. to review the peritoneal macrophages, we inserted them into the wells of 96-well plates at a density of two.0 × 105

cells in an exceedingly volume of 200 µl, which was then incubated for two h (at 37 °C, 5% CO2). The nonadherent fraction was removed, irrigated twice with a fresh medium so allowed incubation for 18 additional hours. NO production was estimated by nitrite content (micromole) within the cell culture supernatants. We added 100 µl of Gris's reagent to 100 µl of supernatant, mixed it and allowed it to incubate for 15 min before measuring the number of reaction product using the “SmartSpec Plus” spectrophotometer (Bio-Rad, USA) at a wavelength of 540 nm.

The study of metabolic characteristics was performed in homogenates of the liver and muscular tissues, taken from the realm of tumour cell inoculation. Samples of right thigh animal tissue and liver were homogenized employing a Potter homogenizer in cold conditions with 2 ml of 0.85% NaCl water solution, containing 0.1% EDTA. Next, we centrifuged the samples for 15 min at 4000 rpm. The carboxylic acid concentration decided using the set of reagents, “Boehringer Mannheim” (Germany). We determined the amount of triglycerides using the set of reagents, “Vector-Best” (Russia). the extent of glycogen was estimated in keeping with the Volchegorsky et al. (2000) method. The activity of arginase and NO was estimated in keeping with the methods described above. to work out NO, we first de-proteinate tissue homogenate by adding 10% acetic acid and so centrifuged the sample for 10 min at 3000 pm. We processed the obtained results using generally accepted methods of variational statistics: dispersion analysis ANOVA and further analysis of batch-to-batch variation using Newman–Keuls test or Mann–Whitney U-test.

Results

After single dosing of carbonate nano-scaled particles, we noted tumour cell necrosis on a periphery of tumour growth and increased content of macrophages during a tumour. Phagosomes with antipsychotic agent particles were revealed within the macrophages' cytoplasm. At the identical time, no tumour cells necrosis was noted in tumour development without lithium influence, mitosis figures were observed, and also the quantitative density of macrophages was 40% lower. during this group of animals,

13 days after the beginning of the experiment, the areas of tumour growth cells were located close and were large in size, and no macrophages were detected in their micro-environment. Determination of blood microvessel volume density in tumours revealed its growth a median of 4.5 times on the third and seventh days of tumour development. Blood microvessel volume density decreased by 40% on the 13th day of the study, exceeding reference level 2.5 times, and increased again by the 30th day of the experiment (Fig. 1).

Fig. 1. Volume density (Vv) of blood microvessels in tumours.

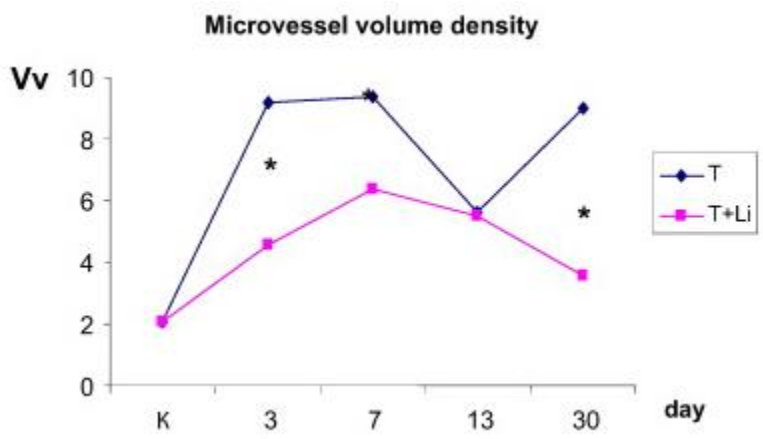

T — tumour; T + Li — 20 days after five-fold injection of Eskalith nano-scaled particles on a periphery of tumour growth. * — $P < 0.05$ compared with a tumour of a bearing group.

Within 30 days post-implantation of hepatocellular carcinoma-29 cells into thighs of experimental animals, the tumour cells formed the likeness of hepatic plates, surrounded by “sinusoids”. Tumour cells were large-sized, had light nuclei with an outsized nucleolus. By the 30th day of study, animals injected with antipsychotic drug nano-scaled particles on a periphery of tumour growth, failed to appear to own plate structure of tumour, had lesser observed vasculature development, the presence of macrophages was retained, and tumour cells with deformed vacuolated nuclei

were noted (Fig. 2).

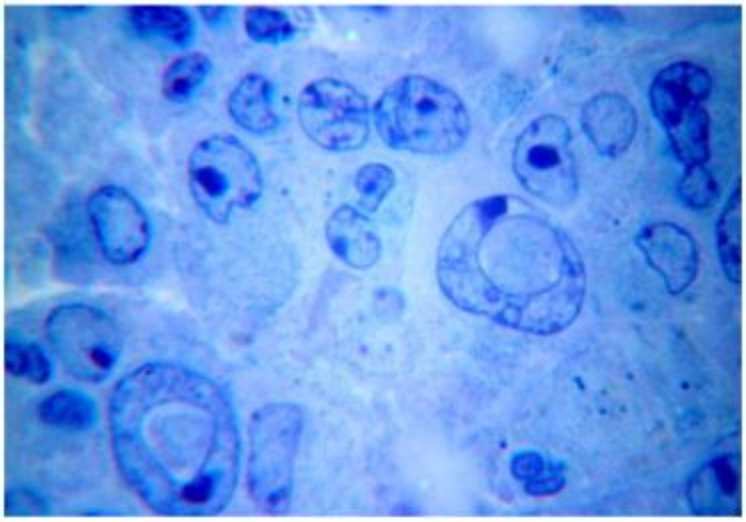

Fig. 2. Deformation of tumour cells' nuclei 20 days after five-fold injection of Eskalith nano-scaled particles. Toluidine blue stain. Magnification: 10 × 90.

In the single-dose lithium nano-scaled particle group, we noted a regional inguinal lymphoid tissue structure with increased secondary lymphoid follicle number, and increased macrophage numeral density (Fig. 3A). Lymphatic sinuses, especially cerebral, were enlarged (Fig. 3B). During 3–15 days of the experiment, we didn't find metastases during a regional inguinal node. The multiple-dose introduction of lithium nano-scaled particles favoured the retention of signs of drainage and detoxification and a rise in organ function, including a substantial dilation of marginal and cerebral sinuses and therefore the growth of macrophages' content in them.

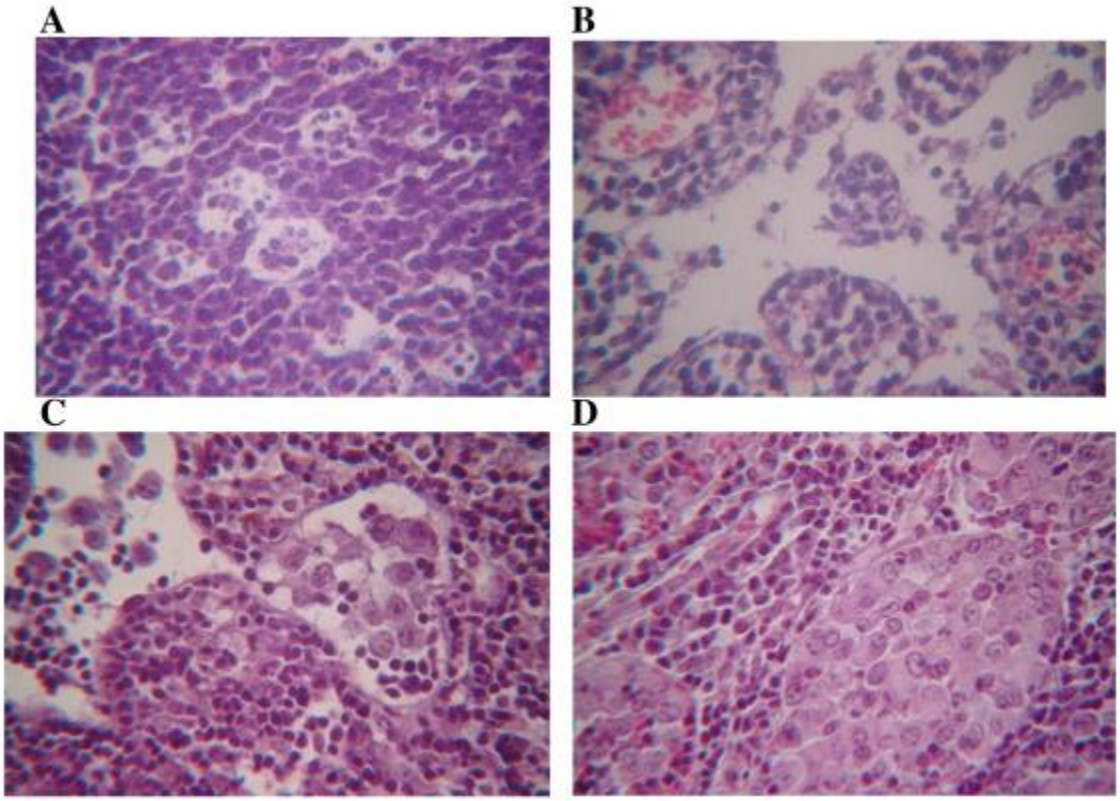

Fig. 3. Structure of a mouse regional inguinal lymphatic tissue after injection of carbonate nano-scaled particles on the periphery of tumour growth. Haematoxylin and eosin stain. Magnification: 10 × 40.

A — Increased content of macrophages within the secondary lymphoid follicle after one dose of lithium nano-scaled particles.

B — Increased sizes of cerebral sinuses after one dose of neuroleptic drug nano-scaled particles.

C — Tumour cells in inguinal lymph gland sinuses at day 30 of the experiment.

D — Replacement of lymphoid parenchyma with tumour cells after 30 days of the ex-

periment.

Thirty days after tumour cell implantation, we found metastases in sinuses and lymphoid parenchyma of regional lymphoid tissue (Fig. 3C, D). Replacement of node structure by tumour cells indicated the event of the lymph's suppression mechanism.

The unexpected structural changes of the lymph glands after injection of lithium nano-scaled particles included the considerable increase of macrophages and neutrophil numbers during tumour development and therefore the conditions of lymph node metastasis. Additionally, blood microvessel volume density was increasing significantly within the area of tumour growth (Fig. 4).

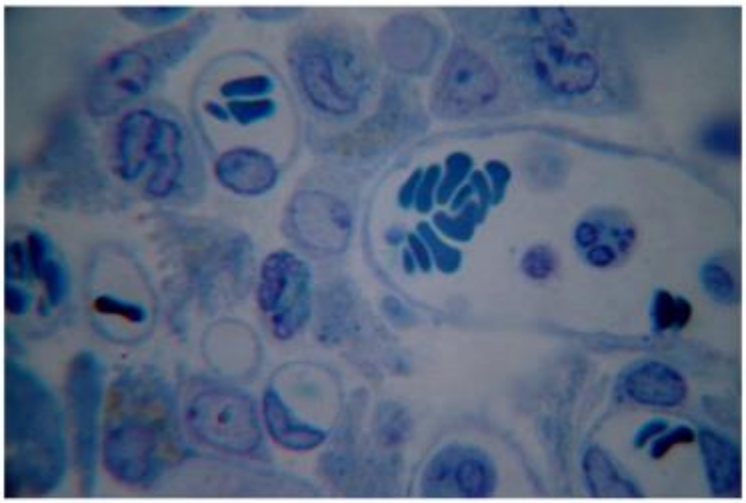

Fig. 4. Tumour cells in inguinal node structure 25 days after the termination of major tranquilizer particles' injection into the region of tumour growth. Increased content of microvessels, macrophages and neutrophils. Toluidine blue stain. Magnification: 10 × 100.

Injection of antipsychotic nano-scaled particles into the tumour growth region set conditions for increasing the macrophage and neutrophil content within the regional structure of the tumour inguinal lymphoid tissue, likewise as intensified destruction of tumour cells and increased the event of vasculature.

After five-fold dosing of lithium nano-scaled particles into the tumour growth region, we noted stasis of erythrocytes in liver sinusoids. In seven days after five-fold dosing of lithium nano-scaled particles into the tumour, local necrosis was observed within the liver. Stasis of erythrocytes and abundance of monocytes and macrophages were also noted. Twenty-five days after five-fold dosing of lithium nano-scaled particles into the tumour, numerous metastases of various sizes (from one to 2 cells up to many dozens of polymorphous cells) were noticed within the liver. additionally to metastases, we also recorded multiple macrophages within the parenchyma; many monocytes, macrophages and neutrophils also filled gaps within sinusoids (Fig. 5).

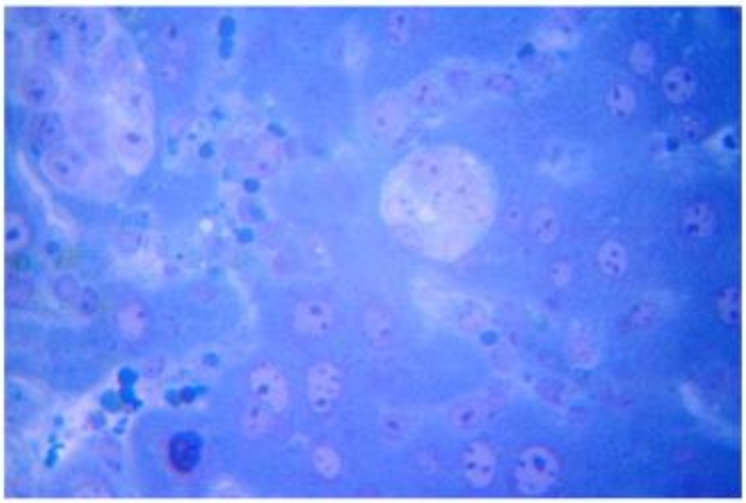

Fig. 5. Metastases of tumour cells in the liver and increased content of macrophages, 30 days after transplantation of hepatocellular carcinoma (H-29) cells into the thigh region of experimental animals, against the background of lithium carbonate nano-scaled particle introduction. Toluidine blue stain. Magnification: 10 × 40.

Under the conditions of major tranquillizer nano-scaled particle introduction into the region of tumour growth with developing carcinoma (H-29), the amount of macrophages grew in liver sinusoids and parenchyma. Within 30 days of the experiment, regions with metastases within the liver were surrounded by an oversized number of macrophages. Lithium injection appears to electrify considerable involvement of macrophages to the liver regions of tumour cell migration.

Correction of tumour process, which is developing in right thigh muscle after inoculation of hepatocarcinoma (H-29) cells, with injections of antipsychotic drug nano-scaled particle suspension directly into affected tissue introduced changes into dynamics of lipid peroxidation processes' activity. Tumour growth in mice under conditions of correction with nano-scaled particles suppressed processes of lipid peroxidation at an early stage and helped prevent spontaneous tumour development (Table 1).

Terms of investigation	Animal groups	
	Tumour	Tumour + Li_2CO_3
Intact	10.86 ± 0.87 (4)	
3 days	4.47 ± 1.37* (4)	5.06 ± 1.46* (4)
7 days	23.2 ± 7.75 (3)	9.64 ± 1.39+ (5)
13 days	15.18 ± 1.37*(4)	10.66 ± 2.12 (4)
33 days	1.79 (1)	3.21 (1)

Comment: the number of animals is included in parentheses.

Table 1. The content of TBA-active products in thigh animal tissue under correction of tumour process by Eskalith nano-scaled particles (M ± m).

Terms of investigation Animal groups
Tumour Tumour + Li2CO3
Intact 10.86 ± 0.87 (4)
3 days 4.47 ± 1.37□ (4) 5.06 ± 1.46□ (4)
7 days 23.2 ± 7.75 (3) 9.64 ± 1.39+ (5)
13 days 15.18 ± 1.37□(4) 10.66 ± 2.12 (4)
33 days 1.79 (1) 3.21 (1)
Comment: the quantity of animals is included in parentheses.

P < 0.05 compared with control.

+P < 0.05 compared with the group of animals with spontaneous tumour development.

However, during subsequent stages of the investigation, the extent of TBA-active products in affected thigh tissue of treated mice returned to the norm. At the identical time, animals with spontaneous tumour development had a major accumulation of lipid peroxidation after products. On day 7, animals that were treated with a five-fold injection of Lithonate nano-scaled particles had 2.4 times less concentration of lipid peroxidation after products compared with indexes, registered for mice with spontaneous tumour development (Table 1). After 13 days, treated animals had the extent of TBA-active products within frames of control values, and it had been 1.4 times less than such index for mice with spontaneous carcinoma development. Thereby, the correction of the tumour process with Lithane nano-scaled particles considerably inhibited the activity of lipid peroxidation processes in tissue affected with hepatoma (H-29).

The development of the tumour process (13th day), both for treated and non-treated animals, was in the course of a rise in catalase activity, which is employed to eliminate oxide from the tumour cells' microenvironment and to extend tumour cells' active proliferation (Table 2).

Terms of investigation	Catalase (U/100 mg)		Superoxide dismutase (U/100 mg)	
	Tumour	Tumour + Li_2CO_3	Tumour	Tumour + Li_2CO_3
Intact	24.9 ± 7.7 (4)		162.9 ± 6.6 (4)	
3 days	23.7 ± 7.3 (4)	36.6 ± 12.6 (4)	152.1 ± 10.4 (4)	138.4 ± 66.1 (4)
7 days	12.1 ± 6.5 (3)	23.7 ± 3.8 (5)	87.9 ± 19.5*(5)	74.9 ± 23.4** (3)
13 days	91.4 ± 12.3*(4)	95.4 ± 12.8* (4)	107.2 ± 38.2 (4)	111.7 ± 35.1 (4)
33 days	31.0 (1)	36.4 (1)	93.1 (1)	135.4 (1)

Comment: the number of animals is stated in parentheses.

Table 2. The content of catalase and enzyme in thigh muscle under correction of tumour process by neuroleptic nano-scaled particles (M ± m).

Terms of investigation Catalase (U/100 mg) Superoxide dismutase (U/100 mg)
Tumour Tumour + Li2CO3 Tumour Tumour + Li2CO3
Intact 24.9 ± 7.7 (4) 162.9 ± 6.6 (4)
3 days 23.7 ± 7.3 (4) 36.6 ± 12.6 (4) 152.1 ± 10.4 (4) 138.4 ± 66.1 (4)
7 days 12.1 ± 6.5 (3) 23.7 ± 3.8 (5) 87.9 ± 19.5□(5) 74.9 ± 23.4□□ (3)
13 days 91.4 ± 12.3□(4) 95.4 ± 12.8□ (4) 107.2 ± 38.2 (4) 111.7 ± 35.1 (4)
33 days 31.0 (1) 36.4 (1) 93.1 (1) 135.4 (1)
Comment: the quantity of animals is stated in parentheses.

$P < 0.05$.

$P < 0.01$ compared with control.

The correction of the tumour process with lithium nano-sized particles failed to influence the amount of catalase activity the least bit stages of the investigation. After seven days postinoculation of carcinoma (H-29) cells into the proper thigh muscle, we

observed a decrease in SOD activity, for treated and non-treated animals, which was successfully overcome in both groups of mice by day 13 of tumour process development (Table 3).

Organs	Terms of investigation				
	Intact (4)	Day 3 (4)	Day 7 (3)	Day 13 (4)	Day 33 (1
Spontaneous development of hepatocellular carcinoma H-29 in the right thigh muscle					
Thigh without tumour	10.86 ± 0.87		5.21 ± 0.76*	3.81 ± 0.62*	1.79
Lungs	8.1 ± 0.77	10.7 ± 1.73	16.42 ± 2.1*	18.13 ± 3.54	22.04
Heart	10.46 ± 2.68	12.1 ± 1.27	16.25 ± 1.05*	11.25 ± 4.13	15.38
Liver	27.21 ± 5.76	11.54 ± 3.05*	16.03 ± 0.53*	16.37 ± 5.47	19.36
Kidneys	25.98 ± 4.46	35.44 ± 7.01	18.64 ± 3.31	20.49 ± 5.53	8.01
Development of hepatocellular carcinoma H-29 in the right thigh muscle under correction by lithium carbonate nano-scaled particles					
Thigh without tumour				3.99 ± 0.89*	1.51
Lungs		22.95 ± 10.04	13.41 ± 2.0	28.54 ± 12.33	13.44
Heart		9.2 ± 2.22	16.31 ± 2.76	12.12 ± 5.42	21.23
Liver		19.33 ± 6.22	20.37 ± 7.04	27.1 ± 9.38	16.0
Kidneys		19.24 ± 3.49	17.15 ± 2.33	22.58 ± 7.69	12.22

Comment: the number of animals is stated in parentheses.

Table 3. The concentration of TBA-active products within the lungs, heart, liver, kidneys and left thigh muscle of mice with hepatoma H-29 development under correction by neuroleptic nano-scaled particles (M ± m).

Organs Terms of investigation

Intact (4) Day 3 (4) Day 7 (3) Day 13 (4) Day 33 (1)

Spontaneous development of hepatoma H-29 within the right thigh muscle

Thigh without tumour 10.86 ± 0.87 5.21 ± 0.76□ 3.81 ± 0.62□ 1.79

Lungs 8.1 ± 0.77 10.7 ± 1.73 16.42 ± 2.1□ 18.13 ± 3.54 22.04

Heart 10.46 ± 2.68 12.1 ± 1.27 16.25 ± 1.05□ 11.25 ± 4.13 15.38

Liver 27.21 ± 5.76 11.54 ± 3.05□ 16.03 ± 0.53□ 16.37 ± 5.47 19.36

Kidneys 25.98 ± 4.46 35.44 ± 7.01 18.64 ± 3.31 20.49 ± 5.53 8.01

Development of hepatoma H-29 within the right thigh muscle under correction by major tranquillizer nano-scaled particles

Thigh without tumour 3.99 ± 0.89□ 1.51

Lungs 22.95 ± 10.04 13.41 ± 2.0 28.54 ± 12.33 13.44

Heart 9.2 ± 2.22 16.31 ± 2.76 12.12 ± 5.42 21.23

Liver 19.33 ± 6.22 20.37 ± 7.04 27.1 ± 9.38 16.0

Kidneys 19.24 ± 3.49 17.15 ± 2.33 22.58 ± 7.69 12.22

Comment: the amount of animals is stated in parentheses.

$P < 0.05$ compared with control.

It is known, that the content of SOD in cells increases in response to increases in superoxide concentration (Menshchikova et al., 2008). Lowered content of enzyme in tumour cells indicates the inhibition of superoxide's intracellular production. It clothed that double-ply and five-fold introduction of antipsychotic agent nano-scaled particles isn't able to sufficiently impact the transformation of intracellular metabolic processes related to the formation and utilization of active oxygen metabolites during tumour development.

During the study of distance effects of major tranquillizer nano-sized particles' multiple-dose introduction under tumour process development, it absolutely was found that dynamic changes of activity of lipid peroxidation processes, registered by the buildup of TBA-active products (malondialdehyde) in several parenchymatous organs — the lungs,

heart, liver and kidney, were in frames of control values (Table 3).

Thus, correction of tumour process by introduction of major tranquillizer nano-scaled particles promoted the defence of significant organs — the guts and lungs, from damaging effect of lipid peroxidation after products. However, the multiple-dose introduction of nano-scaled particles failed to influence the decreased level of lipid peroxidation within the unaffected muscle of the left thigh, with tumour process development within the right thigh muscle. this is often likely to try to to with the particularities of blood-vascular and functioning of lymphatic vessels.

Hydroxyl radical and singlet oxygen is extremely reactive products that may initiate lipid peroxidation. they need enough energy for the discharge and formation of prime lipid radicals, which originate from a rather low-activity superoxide anion-radical, oxide (Menshchikova et al., 2008). Thereby, effects of nano-scaled particles' multiple-dose introduction on lipid peroxidation processes in remote organs, while the tumour process developed within the muscle of the proper thigh, may well be mediated by changing of antioxidant enzymes' activity, which may eliminate initial agents in tissues. Thus, the decrease of catalase activity in muscular tissue under the event of carcinoma (H-29) and with correction using Eskalith nano-sized particles, was significantly less expressed on the third day, whereas the speed of catalase activity within the hearts of treated animals exceeded the speed for non-treated animals 3.4 times.

Organs	Terms of investigation				
	Intact (4)	Day 3 (4)	Day 7 (3)	Day 13 (4)	Day 33 (1)
Spontaneous development of hepatocellular carcinoma H-29 in the right thigh muscle					
Thigh without tumour	24.9 ± 7.7			94.1 ± 11.3*	30.8
Lungs	260.8 ± 36.2	125.7 ± 9.2*	124.8 ± 2.0*	71.21 ± 26.97*	164.8
Heart	52.0 ± 4.6	4.2 ± 0.8*	21.7 ± 8.3*	8.9 ± 3.9*	76.5
Liver	110.7 ± 27.9	51.6 ± 17.4	137.0 ± 13.6	43.9 ± 12.4*	75.2
Kidneys	168.8 ± 24.5	198.5 ± 26.7	21.3 ± 10.3*	246.2 ± 55.3	221
Development of hepatocellular carcinoma H-29 in the right thigh muscle under correction by lithium carbonate nano-scaled particles					
Thigh without tumour				94.08 ± 11.9+	44.89
Lungs		135.2 ± 18.8*	123.7 ± 4.8*+	94.4 ± 11.9*	85.1
Heart		14.4 ± 3.3*+	15.1 ± 4.6*+	15.0 ± 1.7*	70.8
Liver		56.1 ± 19.0	183.9 ± 74.6	58.6 ± 12.0	84.6
Kidneys		202.6 ± 11.2	39.3 ± 21.1*	209.6 ± 42.2	481.9

Comment: the number of animals is stated in parentheses.

Table 4. Catalase activity within the lungs, heart, liver, kidneys and left thigh muscle of mice with carcinoma H-29 development under correction by antipsychotic nano-scaled particles (M ± m).

Organs Terms of investigation

Intact (4) Day 3 (4) Day 7 (3) Day 13 (4) Day 33 (1)

Spontaneous development of carcinoma H-29 within the right thigh muscle

Thigh without tumour 24.9 ± 7.7 94.1 ± 11.3□ 30.8

Lungs 260.8 ± 36.2 125.7 ± 9.2□ 124.8 ± 2.0□ 71.21 ± 26.97□ 164.8

Heart 52.0 ± 4.6 4.2 ± 0.8□ 21.7 ± 8.3□ 8.9 ± 3.9□ 76.5

Liver 110.7 ± 27.9 51.6 ± 17.4 137.0 ± 13.6 43.9 ± 12.4□ 75.2

Kidneys 168.8 ± 24.5 198.5 ± 26.7 21.3 ± 10.3□ 246.2 ± 55.3 221

Development of carcinoma H-29 within the right thigh muscle under correction by major tranquillizer nano-scaled particles

Thigh without tumour 94.08 ± 11.9+ 44.89

Lungs 135.2 ± 18.8□ 123.7 ± 4.8□□ 94.4 ± 11.9□ 85.1

Heart 14.4 ± 3.3□+ 15.1 ± 4.6□□ 15.0 ± 1.7□ 70.8

Liver 56.1 ± 19.0 183.9 ± 74.6 58.6 ± 12.0 84.6

Kidneys 202.6 ± 11.2 39.3 ± 21.1□ 209.6 ± 42.2 481.9

Comment: the amount of animals is stated in parentheses.

$P < 0.05$.

$P < 0.01$ compared with control.

+$P < 0.05$ as compared to animals with spontaneous tumour development.

We didn't register any effects of the treatment on dynamic changes of catalase activity rate within the lungs, liver, kidney and unaffected left thigh muscle under the event of the tumour process (Table 4).

Organs	Terms of investigation				
	Intact (4)	Day 3 (4)	Day 7 (3)	Day 13 (4)	Day 33 (1)
Spontaneous development of hepatocellular carcinoma H-29 in the right thigh muscle					
Thigh without tumour	24.9 ± 7.7			94.1 ± 11.3*	30.8
Lungs	260.8 ± 36.2	125.7 ± 9.2*	124.8 ± 2.0*	71.21 ± 26.97*	164.8
Heart	52.0 ± 4.6	4.2 ± 0.8*	21.7 ± 8.3*	8.9 ± 3.9*	76.5
Liver	110.7 ± 27.9	51.6 ± 17.4	137.0 ± 13.6	43.9 ± 12.4*	75.2
Kidneys	168.8 ± 24.5	198.5 ± 26.7	21.3 ± 10.3*	246.2 ± 55.3	221
Development of hepatocellular carcinoma H-29 in the right thigh muscle under correction by lithium carbonate nano-scaled particles					
Thigh without tumour				94.08 ± 11.9+	44.89
Lungs		135.2 ± 18.8*	123.7 ± 4.8*+	94.4 ± 11.9*	85.1
Heart		14.4 ± 3.3*+	15.1 ± 4.6*+	15.0 ± 1.7*	70.8
Liver		56.1 ± 19.0	183.9 ± 74.6	58.6 ± 12.0	84.6
Kidneys		202.6 ± 11.2	39.3 ± 21.1*	209.6 ± 42.2	481.9

Comment: the number of animals is stated in parentheses.

There was no noted influence of the multiple-dose introduction of lithium nano-scaled particles on the dynamics of SOD activity in remote organs — the lungs, heart, liver, kidney and unaffected left thigh muscle (Table 5).

Table 5. Superoxide dismutase activity in the lungs, heart, liver, kidneys and left thigh muscle of mice with hepatocellular carcinoma H-29 development under correction by lithium carbonate nano-scaled particles (M ± m).

Organs	Terms of investigation				
	Intact (4)	Day 3 (4)	Day 7 (3)	Day 13 (4)	Day 33 (1)
Spontaneous development of hepatocellular carcinoma H-29 in the right thigh muscle					
Thigh without tumour	102.0 ± 37.5			70.5 ± 9.0	151.5
Lungs	788.8 ± 116.7	513.2 ± 58.1	547.2 ± 62.9	736.1 ± 144.8	267.9
Heart	117.7 ± 30.7	133.1 ± 21.6	75.6 ± 13.98	56.34 ± 5.41	12.0
Liver	92.07 ± 21.34	144.1 ± 70.1	77.88 ± 40.53	171.25 ± 39.5	119.5
Kidneys	142.4 ± 22.02	372.4 ± 40.6*	356.5 ± 22.46*	483.0 ± 81.4*	393.8
Development of hepatocellular carcinoma H-29 in the right thigh muscle under correction by lithium carbonate nano-scaled particles					
Thigh without tumour				60.3 ± 28.45	140.6
Lungs		654.1 ± 218.3	439.7 ± 98.37	674.1 ± 161.19	204.2
Heart		125.6 ± 21.92	57.21 ± 5.19	69.68 ± 7.8	228.0
Liver		72.12 ± 36.3	134.5 ± 61.8	187 ± 19.5	79.83
Kidneys		366.1 ± 16.74*	367.7 ± 50.72**	409.2 ± 68.68*	621.5

Comment: the number of animals is stated in parentheses.

Table 5. SOD activity within the lungs, heart, liver, kidneys and left thigh muscle of mice with carcinoma H-29 development under correction by antipsychotic nano-scaled particles (M ± m).

Organs Terms of investigation
Intact (4) Day 3 (4) Day 7 (3) Day 13 (4) Day 33 (1)
Spontaneous development of malignant hepatoma H-29 within the right thigh muscle
Thigh without tumour 102.0 ± 37.5 70.5 ± 9.0 151.5
Lungs 788.8 ± 116.7 513.2 ± 58.1 547.2 ± 62.9 736.1 ± 144.8 267.9
Heart 117.7 ± 30.7 133.1 ± 21.6 75.6 ± 13.98 56.34 ± 5.41 12.0
Liver 92.07 ± 21.34 144.1 ± 70.1 77.88 ± 40.53 171.25 ± 39.5 119.5
Kidneys 142.4 ± 22.02 372.4 ± 40.6□ 356.5 ± 22.46□ 483.0 ± 81.4□ 393.8

Development of hepatocarcinoma H-29 within the right thigh muscle under correction by antipsychotic agent nano-scaled particles
Thigh without tumour 60.3 ± 28.45 140.6
Lungs 654.1 ± 218.3 439.7 ± 98.37 674.1 ± 161.19 204.2
Heart 125.6 ± 21.92 57.21 ± 5.19 69.68 ± 7.8 228.0
Liver 72.12 ± 36.3 134.5 ± 61.8 187 ± 19.5 79.83
Kidneys 366.1 ± 16.74□ 367.7 ± 50.72□□ 409.2 ± 68.68□ 621.5
Comment: the quantity of animals is stated in parentheses.

$P < 0.05$.

$P < 0.01$ compared with control.

Thereby, the introduction of major tranquillizer nano-scaled particles into the thigh muscle caused a rise in lipid peroxidation activity in animal tissue. This led to the alteration within the tissue and also the development of inflammatory infiltration, as indicated by a rise in tissue protein concentration. After the event of an inflammatory response to the introduction of neuroleptic agent nano-scaled particles, there was a secondary increase in lipid peroxidation activity, resulting in a secondary alteration. This secondary altera-

tion included a control of the discharge of lysosomal enzymes and active oxygen metabolites from cells, in animal tissue and microvessels. The introduction of Eskalith nano-scaled particles provoked the enhancement of catalase activity, which led to dynamic changes of lipid peroxidation intensity and a decrease of SOD activity.

Evaluation of haemoglobin concentration revealed that on the third day of carcinoma development, the content of haemoglobin within the affected muscle of treated mice was twice higher compared with the reference level. At the identical time, the content of haemoglobin for untreated mice didn't change from the reference level (Table 6).

Table 6. Changes in haemoglobin concentration within the thigh muscle of mice with carcinoma H-29 development under correction by neuroleptic drug nano-scaled particles (M ± m).

Organs Terms of investigation
Intact Day 3 (4) Day 7 Day 13 Day 3
Thigh without tumour 0.57 ± 0.09 (4) 0.19 (1)
Thigh with tumour 0.68 ± 0.09□ (4) 0.47 ± 0.04□□ (5) 0.67 ± 0.12□ (4) 0.22 (1)
Comment: the quantity of animals is stated in parentheses.
However, the tumour's systemic action on haemoglobin levels in unaffected muscle of the left thigh at the late stages (13th day) disappeared under treatment. this can be possibly indicative of nano-scaled particles indirect effects on decreasing the assembly of VEGF-A, therefore affecting circulation.

Multiple-dose introduction of Lithane nano-scaled particles possibly contribute to the lower level of vascularisation of carcinoma (H-29) fast-growing tumour node in animal tissue. This conclusion relies on the dearth of serious difference between the content of carboxylic acid for treated animals from the reference values on the 13th day, whereas non-treated animals had a carboxylic acid index significantly not up to reference val-

ues (Table 7).

Table 7. Change of lactate concentration in the thigh muscle of mice with spontaneous hepatocellular carcinoma H-29 development and under correction by lithium carbonate nano-scaled particles (M ± m).

Animal groups	Stages of investigation			
	Intact	Day 3 (4)	Day 13	Day 3
Spontaneous development	2.33 ± 0.05 (4)	3.50 ± 0.63 (4)	1.33 ± 0.11* (4)	2.18 (1)
Under correction by lithium carbonate nano-scaled particles		4.91 ± 2.25 (4)	1.61 ± 0.37 (4)	2.79 (1)

Comment: the number of animals is stated in parentheses.

Table 7. Change of lactate concentration within the thigh muscle of mice with spontaneous hepatocarcinoma H-29 development and under correction by Eskalith nano-scaled particles (M ± m).

Animal groups Stages of investigation
Intact Day 3 (4) Day 13 Day 3
Spontaneous development 2.33 ± 0.05 (4) 3.50 ± 0.63 (4) 1.33 ± 0.11□ (4) 2.18 (1)
Under correction by antipsychotic nano-scaled particles 4.91 ± 2.25 (4) 1.61 ± 0.37 (4) 2.79 (1)
Comment: the quantity of animals is stated in parentheses.

□

P < 0.05 compared with control.

Hereby, the fast growth of vessels which supply the tumour results in a decrease of carboxylic acid accumulation in affected muscle.

Two-fold introduction of antipsychotic agent nano-scaled particles reliably increased the amount of gas production by peritoneal macrophages on day 3 of tumour process development in thigh muscle (Fig. 6).

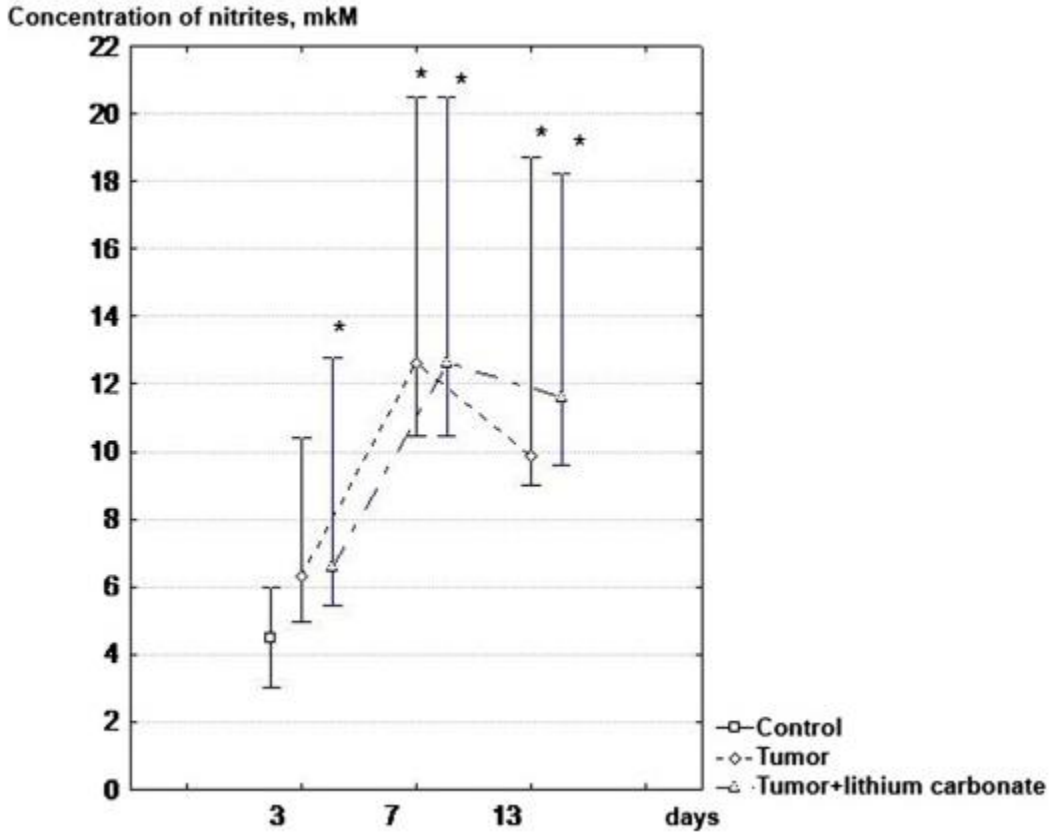

Fig. 6. Dynamics of NO production by peritoneal macrophages, with malignant hepatoma (H-29) development within the animal tissue of right thigh under conditions of correction using neuroleptic agent nano-scaled particles. * — $P < 0.05$ compared with the

group of intact animals.

Table 6. Changes of haemoglobin concentration in the thigh muscle of mice with hepatocellular carcinoma H-29 development under correction by lithium carbonate nano-scaled particles (M ± m).

Organs	Terms of investigation				
	Intact	Day 3 (4)	Day 7	Day 13	Day 3
Thigh without tumour				0.57 ± 0.09 (4)	0.19 (1)
Thigh with tumour		0.68 ± 0.09* (4)	0.47 ± 0.04** (5)	0.67 ± 0.12* (4)	0.22 (1)

Comment: the number of animals is stated in parentheses.

After the introduction of antipsychotic nano-scaled particles, our results show that the dynamics of carboxylic acid and triglycerides' content was changing within the area of the muscle inoculated by tumour cells. In cases of hepatocarcinoma development without the influence of lithium, lipid accumulation in muscle occurs slowly, growing by the 13th day. In contrast, triglyceride levels in treated mice on the third day after tumour process induction increased 4.7 times compared with the reference values, which also exceeded rates within the biological group without impact by 1.7 times (Fig. 7). This finding correlates with previous research showing that after the addition of conjugated polyunsaturated fatty acid to hepatoma HepG2 culture, the inhibition of tumour cell proliferation was among a rise in intracellular lipids (triglycerides, total cholesterol, free cholesterol) and carboxylic acid concentration (Igarashi and Miyazawa, 2001). These results taken together show that changes within the metabolism of fatty acids influenced the intensity of tumour cells proliferation.

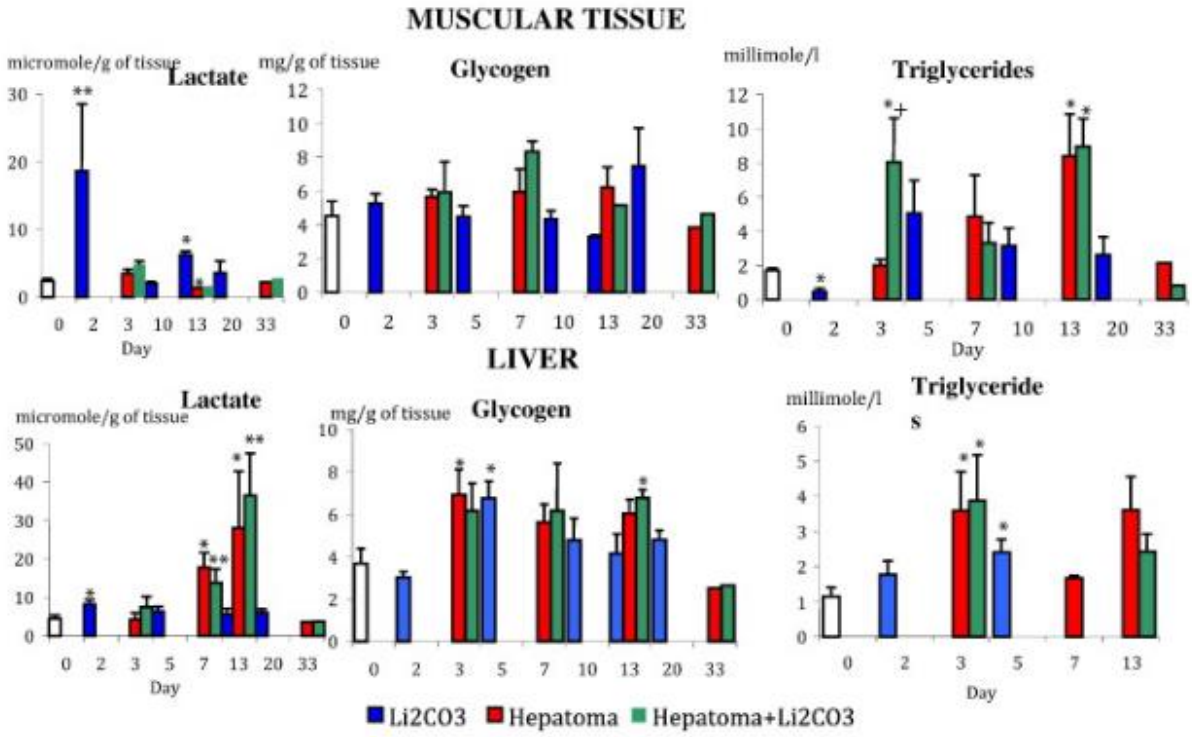

Fig. 7. Metabolic changes in muscle and liver under conditions of tumour growth and impact of Lithonate nano-scaled particles.

— $P < 0.05$ compared with control.

Lactic acid concentrations within the liver increased gradually in animals with spontaneous development of tumour process in muscle caused by the inoculation of hepatocarcinoma cells. On the 7th day of hepatocarcinoma development, the concentration of lactate within the liver exceeded control values 3.9 times, and on the 13th day, it exceeded control values 6.2 times (Fig. 7). This argued for activation of the anaerobic glycolysis process and therefore the development of anaemia hypoxic syndrome. Under conditions lacking oxygen, mitochondrial inhaling cells reduces and ATP is produced by anaerobic glycolysis. Hypoxia-inducible factor, a regulator of transcrip-

tion for glucose metabolism enzymes (Pescador et al., 2010), plays a key role during this metabolic shift. within the liver, lactate usually turns into glucose, then through glycogenesis turns into glycogen. During our experiment, the extent of glycogen almost doubled — becoming 1.9 times higher compared with the reference level from day three of hepatoma development (Fig. 7). The study showed that hypoxia can cause the buildup of glycogen by enhancement of glucose flux within the cell. this happens because of a rise within the level of a transporter protein, GLUT-1 and glucose's participation in its biosynthesis by activation of glycogen synthase (Pescador et al., 2010). This mechanism is confirmed by cell culture studies, which were performed on myocytes, normal hepatocytes and cells of various hepatomas. Glycogen accumulation in cells improves their survivability under hypoxia. During subsequent time points in our study, the extent of glycogen in liver tissue failed to significantly differ from the control group.

This study has shown that excess glucose enters into the circulation and was consumed more not by the tumour tissue, but by other tissues because their metabolism switched to glucose's consumption because of lack of oxygen provision. Also, excess glucose was likely converted into triglycerides by the liver, as seen by the day three concentration of triglycerides being 3.1 times above its rate within the group of intact animals. Triglyceride accumulation in muscle within the area inoculated by tumors cells can even be explained by significant decreases in lipase, which decomposes neutral fats. Patients with carcinoma development experience damage to liver cells, and therefore the activity of lipase, which hydrolyses triglycerides, goes down (Hiraoka et al., 1993). Correction of hepatocellular carcinoma-29, developing in animal tissue, by neuroleptic nano-scaled particles didn't influence the intensity of anaerobic glycolysis or accumulation of glycogen and triglycerides within the liver because the dynamics of lactate, glycogen and triglycerides concentration was the identical as for animals with spontaneous tumour development (Fig. 7).

CONCLUSION

During the primary fortnight of tumour process development within which antipsychotic drug nano-scaled particles were introduced, we monitored the activation of the drainage-detoxification function of regional to tumour lymphatic tissue and metabolic processes in muscle and liver. Under conditions of tumour process progression, the protective barrier functions of the lymph nodes gradually decreased. By the 30th day of the experiment, tumour cells disseminated into regional lymph nodes and also the liver. Single and multiple doses of antipsychotic nano-scaled particles on the periphery of tumour growth failed to end in the removal of tumour cells from the thigh muscle. We also noted within the early stages after the introduction that there was a rise of macrophages and neutrophils within the tumour, a decrease in blood microvessel density and haemoglobin and a rise of tumour cell necrosis rate. Then, within the late stages of tumour development, there have been destructive changes occurring within the cytoplasm and nuclei of tumour cells. During tumour process development, neither one nor five-fold introduction of lithium nano-scaled particles affected NO production by peritoneal macrophages. Correction of tumour process by neuroleptic agent nano-scaled particles inhibited the activity of lipid peroxidation processes in tissue which was tormented by hepatoma by inoculation. However, it failed to impact the activity of antioxidant enzymes like catalase and SOD. The introduction of neuroleptic nano-scaled particles into the world of tumour growth protected vital organs like the center and lungs from the damaging effect of lipid peroxidation after products.

REFERENCES

Bgatova et al., 2012
N.P. Bgatova, O.P. Makarova, A.A. Pozhidayeva, Y.I. Borodin, L.N. Rachkovskaya, V.I. Konenkov
Biological effects of lithium nano-scaled particles
Achiev. Life Sci., 5 (2012), pp. 29-46
Google Scholar

Canales et al., 1999
M.A. Canales, R. Arrieta, C. Hernandez-Garcia, J.G. Bustos, M.J. Aguado, F. Hernandez-Navarro
Single apheresis to realize a high number of peripheral blood CD34+ cells during a lithium-treated patient with acute myeloid leukaemia
Bone Marrow Transplant., 23 (3) (1999), p. 305-305
Google Scholar

Corraliza et al., 1994
I.M. Corraliza, M.L. Campo, G. Soler, M. Modolell
Determination of arginase activity in macrophages: a micro method
J. Immunol. Methods, 174 (1994), pp. 231-235
ArticleDownload PDFView Record in ScopusGoogle Scholar

Golokhvastov et al., 2013
K.S. Golokhvastov, N.P. Bgatova, V.V. Seagull, A.M. Panichev, F.N. Gulkov
Effect of nano and microparticles zeolites on the reaction for various routes of administration
Russ. Immunol. J., 7 (2–3) (2013), pp. 183-184
Google Scholar

Hager et al., 2001
E.D. Hager, H. Dziambor, D. Hohmann, P. Winkler, H. Strama
Effects of lithium on thrombopoiesis in patients with low platelet cell counts following chemotherapy or radiotherapy
Biol. Trace Elem. Res., 83 (2) (2001), pp. 139-148
View Record in ScopusGoogle Scholar

Hager et al., 2002
E.D. Hager, H. Dziambor, P. Winkler, D. Hohmann, K. Macholdt

Effects of Lithane on hematopoietic cells in patients with persistent neutropenia following chemotherapy or radiotherapy
J. Trace Elem. Med. Biol., 16 (2) (2002), pp. 91-97
ArticleDownload PDFView Record in ScopusGoogle Scholar

Hiraoka et al., 1993
H. Hiraoka, S. Yamashita, Y. Matsuzawa, M. Kubo, S. Nozaki, N. Sakai, K. Hirano, S. Kawata, S. Tarui
Decrease of hepatic triglyceride lipase levels and increase of cholesteryl ester transfer protein levels in patients with primary biliary cirrhosis: relationship to abnormalities in HDL Hepatology, 18 (1) (1993), pp. 103-110
View Record in ScopusGoogle Scholar

Igarashi and Miyazawa, 2001
M. Igarashi, T. Miyazawa
The growth inhibitory effect of conjugated linolic acid on somebody's hepatoma cell line, HepG2, is induced by a change in carboxylic acid metabolism, but not the facilitation of lipid peroxidation within the cells
Biochim. Biophys. Acta, 1530 (2–3) (2001), pp. 162-171
ArticleDownload PDFView Record in ScopusGoogle Scholar

Kaledin et al., 2009
V.I. Kaledin, N.A. Zhukova, V.P. Nikolin, I.A. Popova, M.D. Belyaev, N.V. Baginskaya, E.A. Litvinova, T.G. Tolstikova, E.L. Lushnikova, D.E. Semenov
Hepatocellular carcinoma-29 — metastasizing transplantable mice's tumour calling cachexia
Bull. Exp. Biol. Med., 148 (12) (2009), pp. 664-669
View Record in ScopusGoogle Scholar

Khasraw et al., 2012
M. Khasraw, D. Ashley, G. Wheeler, M. Berk
Using lithium as a neuroprotective agent in patients with cancer
BMC Med., 10 (131) (2012), pp. 1-7

Google Scholar
Kudo, 2012
M. Kudo
Treatment of advanced malignant hepatoma with emphasis on hepatic arterial infusion chemotherapy and molecular targeted therapy
Liver Cancer, 1 (2) (2012), pp. 62-70
CrossRefView Record in ScopusGoogle Scholar

Lee et al., 2014
J.E. Lee, S.H. Bae, J.Y. Choi, S.K. Yoon, Y.K. You, M.A. Lee
Epirubicin, Cisplatin, 5-FU combination chemotherapy in sorafenib-refractory metastatic hepatocarcinoma
World J. Gastroenterol., 20 (1) (2014), pp. 235-241
View Record in ScopusGoogle Scholar

Lowry et al., 1951
O.H. Lowry, N.J. Rosebrough, A.L. Farl, R.J. Randall
Protein measurement with the Folin phenol reagent
J. Biol. Chem., 193 (1) (1951), pp. 265-275
ArticleDownload PDFView Record in ScopusGoogle Scholar

Menshchikova et al., 2008
E.B. Menshchikova, N.K. Zenkov, V.Z. Lankin, I.A. Bondar, V.A. Trufakin
Oxidative Stress: Morbid Condition and Diseases
Artra, Novosibirsk (2008)

Google Scholar

Merendino et al., 1994
R.A. Merendino, G. Mancuso, F. Tomasello, D. Gazzara, V. Cusumano, S. Chillemi, P. Spadaro, M. Mesiti
Effects of neuroleptic drug on cytokine production in patients laid low with carcinoma
J. Biol. Regul. Homeost. Agents, 8 (3) (1994), pp. 88-91
View Record in ScopusGoogle Scholar

Mo et al., 2012
M. Mo, I. Erdelyi, K. Szigeti-Buck, J.H. Benbow, B.E. Ehrlich
Prevention of paclitaxel-induced peripheral neuropathy by lithium pretreatment
FASEB J., 26 (11) (2012), pp. 4696-4709
CrossRefView Record in ScopusGoogle Scholar

Nepomnyashchikh et al., 2005
L.M. Nepomnyashchikh, E.L. Lushnikova, O.P. Molodykh, M.G. Klinnikova
Ultrastructural manifestations of cardiac histiocytes regeneration disturbance under the effect of doxorubicin
Morphology, 4 (2005), pp. 81-84
Google Scholar

Nepomnyashchikh et al., 2006
L.M. Nepomnyashchikh, E.L. Lushnikova, O.P. Molodykh, M.G. Klinnikova
Structural reorganization of rats' livers under cytotoxic action of doxorubicin
Bull. Exp. Biol. Med., 141 (5) (2006), pp. 579-585
Google Scholar

Pang and Poon, 2012
R.W. Pang, R.T. Poon

Cancer somatic cell as a possible therapeutic target in hepatocarcinoma
Curr. antineoplastic Targets, 1 (2(9)) (2012), pp. 1081-1094
View Record in ScopusGoogle Scholar

AUTHOR AFFILIATION

AKOM PEMMANUEL NUJOR
ABUOH RIDELIS KOSOMKO